Probing Amplitude, Phase, and Polarization of Microwave Field Distributions in Real Time

R. J. KING, SENIOR MEMBER, IEEE, AND Y. H. YEN

Abstract—**A coherent (homodyne) detection system is used to map field distributions in real time. A key feature is the use of an electrically modulated (10-kHz) dipole scatterer which is also mechanically spun (150 Hz) to create an amplitude- and phase-modulated backscattered field. The system is monostatic. The backscattered field is coherently detected by mixing with the CW reference. A phase-insensitive detector is used, comprised of two balanced mixers which are fed in quadrature phase by one of the RF inputs followed by a phase quadrature combiner. The resulting amplitude and phase of the 10-kHz output are proportional to the square of the RF field component along the instantaneous axis of the spinning dipole. Both are measured simultaneously and independently in real time. From these, the polarization properties can also be found, so the field is uniquely described. The system's application to scanning the *E*-field transmitted through lossy, nonhomogeneous and anisotropic media (e.g., wood) is demonstrated. Other applications besides nondestructive testing are microwave vector holography, near-field antenna measurements, and inverse scattering.**

I. Introduction

NEAR-FIELD antenna measurements, microwave vector holography, inverse scattering, and nondestructive testing are but a few emerging technologies which require that the field be uniquely measured over large areas. Uniqueness, of course, implies that the amplitude, phase, and vector properties of the tangential fields (either $\boldsymbol{E}$ or $\boldsymbol{H}$) must be recorded over a surface. Ideally, this should be done with a single-point probe which does not disturb the field, making probe corrections unnecessary or minimal. While the RF circuitry usually associated with the probe (e.g., cables, waveguides, mixers, receiver, etc.) can generally be shielded with absorbers to minimize field disturbances, the amount of such circuitry should be minimal from the standpoints of cost, convenience, and simplicity. Moreover, the measurement system should be highly sensitive and linear over a wide dynamic range.

These needs are largely fulfilled by using a small scattering dipole probe which is electrically modulated at f_m (typically several kilohertz), in conjunction with a special coherent detection system for detecting the scattered field. The backscattered field is proportional to the square of the component of the complex phasor field aligned with the dipole. Thus since coherent (homodyne) detectors are phase sensitive, the phase as well as the amplitude information contained in the backscattered field is preserved. The vector information can be obtained by spinning the dipole at frequency f_s (typically a few hundred hertz) in the tangent plane of the surface being scanned.

The detector is configured so that amplitude, phase, and polarization properties are available simultaneously and independently in real time at a rate $2f_s$. Another important advantage is that the IF is zero so that all signal processing can be done at the audio frequencies, f_m and $2f_s$.

The use of electrically modulated scattering dipoles in conjunction with homodyne detection techniques to measure $\boldsymbol{E}$ or $\boldsymbol{H}$ field distributions is certainly not new. Neither is the use of mechanically spun dipoles new. The history, theory, and application of this technology are thoroughly discussed in a recent book [1]. What is new here is that both electrical *and* mechanical modulation are used simultaneously to uniquely characterize the measured field in real time. The principles and techniques described in the following is the subject of a recent U.S. patent [2].

If the vector nature of the field is known *a priori* (e.g., the field is known to be linearly polarized), the spinning part of the probe modulation is unnecessary. But more generally, both modulations are needed when measuring arbitrarily polarized fields (e.g., fields which are elliptically polarized by reflection, refraction, or diffraction). The greatest versatility of the system is realized when measuring fields which are the combination of *two* elliptically polarized waves, such as those created by reflection, refraction, or diffraction via anisotropic media.

II. The Microwave Instrumentation

The basic instrumentation and the scattering dipole are shown in Fig. 1. Heavy dark lines denote the paths of microwave (RF) power flow and lighter lines denote AF signal paths. The CW source at frequency ω typically has an output of about 2 W. Most of this power is split by the magic tee so that about 1 W is radiated by the transmitting antenna at port 3. The other half is dissipated in the Z_0 termination at port 2 and serves no useful purpose. Tuner T_3 is adjusted to minimize the power at the isolated port 4, as measured by temporarily connecting a power meter.

A few milliwatts of CW power is also diverted to the balanced mixers via the RF probe in the slotted line. This

Manuscript received April 6, 1981; revised June 29, 1981. This work was supported by the U. S. Forest Service, Forest Products Laboratory, under Grant FS-FPL-3501, the Weyerhaeuser Co., and the University of Wisconsin Research Committee.

The authors are with the Department of Electrical and Computer Engineering, University of Wisconsin, Madison, WI 53706.

0018-9480/81/1100-1225$00.75 ©1981 IEEE

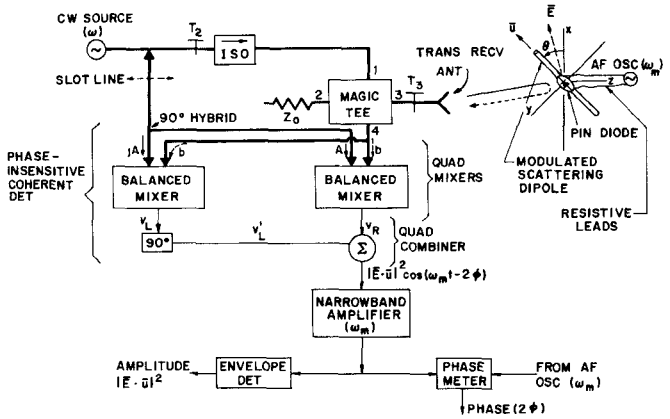

Fig. 1. Basic microwave homodyne detection system and modulated scattering dipole.

serves as the reference signal (i.e., the local oscillator in heterodyne terminology) for the homodyne mixers. Tuner T_2 is adjusted for a "flat" slotted line such that the phase of the reference signal is linearly proportional to the position of the slotted line probe. This is a simple and effective means of varying the RF phase for calibration purposes, and for choosing the reference phase for relative phase measurements.

The dipole probe is electrically modulated at ω_m by switching a p-i-n- diode connected to its terminals as the load impedance Z_L. The modulating voltage from an AF sinusoidal oscillator is fed to the diode via resistive leads which are essentially transparent to the RF so that the field is minimally disturbed.

The Appendix briefly reviews the theory of scattering from a modulated dipole. There, it is shown that the relevant backscattered voltage appearing at the transmit–receive antenna port is proportional to the modulated phasor

$$\Delta V = C|\boldsymbol{E}_1 \cdot \boldsymbol{u}(t)|^2 (1 + m\cos\omega_m t) e^{-j2\phi(t)} \tag{1}$$

where $|\boldsymbol{E}_1 \cdot \boldsymbol{u}(t)|$ and $\phi(t)$ are the instantaneous amplitude and phase, respectively, of the component of $\boldsymbol{E}_1$ in the direction of $\boldsymbol{u}(t)$, i.e., parallel to the instantaneous axis of the dipole. This voltage is split by the magic tee, so that half of the power emerges at port 4 and the other half emerges at port 1 where it is dissipated in the isolator. Further, that half from port 4 is split by a tee such that the waves arriving at the two balanced mixers (denoted as b in Fig. 1) are in phase.

The reference signal power which is diverted via the slotted line is split by a quadrature tee (e.g., a quadrature 3-dB coupler or 90° hybrid) such that symmetry is preserved except for a phase shift of $\pi/2$, in say the left branch. Thus the reference voltages are fed to the left and right mixers are

$$e_L = je_R = jAe^{j\omega t} \tag{2}$$

and the information signal to either mixer is (1) multiplied by $\exp(j\omega t)$

$$e_i = C|\boldsymbol{E} \cdot \boldsymbol{u}(t)|^2 (1 + m\cos\omega_m t) e^{j[\omega t - 2\phi(t)]}. \tag{3}$$

Assuming that A is large (typically 1–10 dBm) so that the mixers operate as linear envelope detectors, the homodyne ω_m output of the one on the right is

$$V_R = K_R|\boldsymbol{E} \cdot \boldsymbol{u}|^2 \cos 2\phi \cos\omega_m t \tag{4a}$$

and

$$V_L = -K_L|\boldsymbol{E} \cdot \boldsymbol{u}|^2 \sin 2\phi \cos\omega_m t \tag{4b}$$

for the left mixer, where K_L and K_R are the mixer conversion factors. These outputs are fed to a quadrature combiner which shifts one of them by 90° (say V_L as in Fig. 1), and combines both of them giving

$$V_T = V_R + V_L' = K|\boldsymbol{E} \cdot \boldsymbol{u}(t)|^2 \cos\left[\omega_m t - 2\phi(t)\right] \tag{5}$$

if $K_L = K_R$, and K is an overall conversion constant. After amplification and filtering to eliminate all unwanted frequencies and retaining only the $\omega_m \pm n\omega_s$ terms, the instantaneous mean square of the amplitude can be measured using an envelope detector. The instantaneous round-trip RF phase, $2\phi(t)$, is measured at ω_m by an analog phase meter or by a digital computer, using the ω_m reference from the AF oscillator. Thus the instantaneous amplitude and phase are available in real time, simultaneously and independently. Contrast (5) with the output of a single mixer, (4a) or (4b), which contain phase-sensitive amplitude factors $\cos 2\phi$ or $\sin 2\phi$. Hence, we term the detection circuitry in Fig. 1 as a *phase-insensitive coherent (homodyne) detector*. It has the same form as a well-known circuit for *single-sideband modulation* of a CW carrier, except that, in the present case, it is being used as a detector of one (upper) sideband. The lower sideband results if the quadrature combiner subtracts rather than adds the two ω_m inputs. This circuit also has the same form as an *image rejection mixer* commonly used in heterodyne detection to give the upper or lower sidebands at the intermediate frequency (IF). Unfortunately, the IF of available image-rejection mixers is of the order of a few megahertz and up. For the present application where the IF is zero and f_m is only a few kilohertz, a specially designed quadrature combiner is necessary. The quadrature mixers are readily available in strip-line packages. Waveguides or coaxial versions can also be used [1].

Apparently, Kalmus [3] was the first to apply this detector circuit in a coherent mode in 1955, where it was used in a direction-sensitive Doppler radar. More recently, Koelle and Depp [4] extended its use to cooperative targets in which the backscattered signal is modulated at ω_m (as is done here), apparently without knowledge of Kalmus' paper. Koelle *et al.* [5] also used it in a telemetry system for measuring the amplitude of the signal backscattered from a coded modulated scatterer. Still other applications are described by King [1, chs. 10 and 12].

Analysis of phase and amplitude errors of the phase-insensitive detector are given elsewhere [6]. It is sufficient to remark that errors due to quadrature phase or amplitude unbalance between the two mixers can be totally mitigated by careful design and trim adjustment of the combiner. The only errors which cannot be reduced to inconsequen-

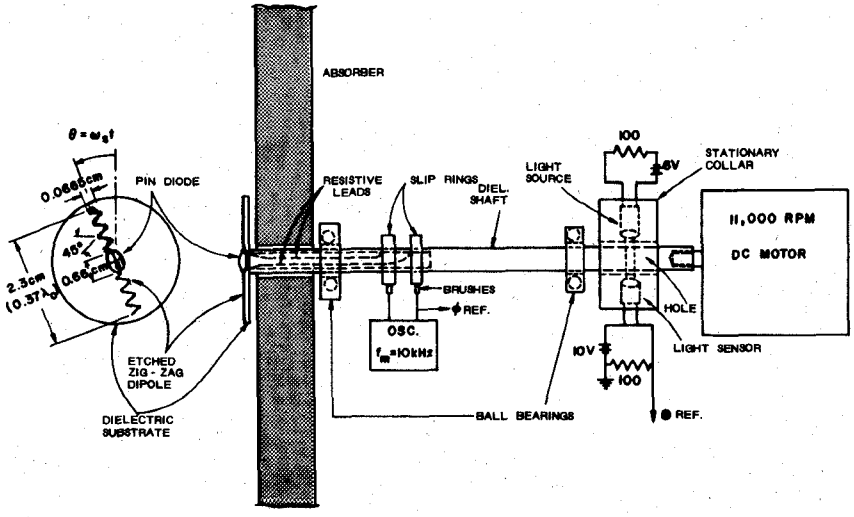

Fig. 2. Electrically modulated and mechanically spun scattering dipole.

tial levels are those inherent to the detection process itself. They arise when the carrier (ω) in the information channel is comparable to A. For this reason, the balanced mixers should be of the 180° variety which suppress the unwanted carrier, typically by a factor of 20 to 30 dB. The first term in (3) represents such an unwanted carrier, but it is normally quite small and presents no problems. Much more troublesome are unwanted reflections from objects in the foreground of the transmit–receive antenna, or from the antenna itself. As noted earlier, tuner T_3 is used to minimize this unwanted carrier.

III. The Scattering Dipole

The "probe" is an electrically modulated zig-zag dipole which is spun at 11 000 r/min (Fig 2). The dipole is a printed circuit etched on a dielectric substrate to provide mechanical rigidity and balance. A p-i-n diode serves as the load impedance Z_L, switched at 10 kHz, fed from an external oscillator via brushes, slip-rings, and resistive leads. These leads are essentially transparent to the RF field, but are sufficiently conductive ($\simeq 0.6$ kΩ/cm per line) to provide 1–2 V at the diode terminals. They are commercially available filaments of polytetraflouroethylene rendered semiconducting by uniformly dispersing fine carbon particles through the plastic while in its semifluid state. The lines are drawn in 0.03-in filaments, and coated with a 0.005-in nylon film for strength and insulation. The leads are bonded to the diode and slip ring using silver paint.

A zigzag design is used because the resonant length of the dipole is significantly less than $\lambda_0/2$. Tuning is accomplished by symmetrically trimming away both ends a bit at a time, while the modulated probe is positioned in the RF field, observing the output of the homodyne detector. Resonance is achieved for a length of about 0.37 λ_0.

Polarization angle, Θ, measurements require knowing the dipoles instantaneous rotation angle ($\theta(t)=\omega_s t$). This requires that a Θ-reference pulse be generated, say at $\theta=0$ and π. To do this, a stationary collar is mounted around the shaft which has a small hole in its diameter. A light emitter and sensor are diametrically positioned in the collar so that a pulse is sensed when the hole in the shaft is aligned with the emitter–sensor pair. This reference pulse is then hard-clipped and used to time the position (θ) of a maximum in the detected backscattered field.

The entire mechanism in Fig. 2 is covered with microwave absorbing material and mounted on a small movable nonmetal platform (not shown). The probe is scanned vertically by a programmable stepping motor. It is not yet instrumented for horizontal scanning.

IV. Analog Signal Processing

Fig. 3 shows the entire system, as used for nondestructive testing of wood. This application is useful to illustrate the system's operation, but the analog-signal-processing portion is sufficiently general for use in most other applications. Various other circuits may serve as well. The digital processing portion is somewhat unique to this application, so only its general operation will be discussed without detail.

Wood is nonhomogeneous, lossy, and anisotropic. Consequently, the amplitude, phase, and polarization properties of the field transmitted through the wood are diagnostic indicators of the wood's physical properties, i.e., moisture content, density, and grain angle [7]. Grain orientation and moisture content are critical parameters in producing high-grade dimension lumber, and in the laminating industry. For example, the structural strength of wood under bending stress is chiefly determined by the grain direction. Knowing the moisture content would be of great benefit in estimating drying requirements, or determining whether the wood is suitable for processing, as in the manufacture of veneer and particle board.

In this example, the spinning dipole is positioned very close to the wood ($\lambda_0/6$ to $\lambda_0/3$) so as to measure the integrated field over a local area of the order of λ_0^2. The wood moves horizontally between the transmit–receive horn antenna and the spinning dipole, and the dipole can be scanned in vertical steps. The incident field is vertically polarized, but the polarization of the backscattered field is a function of the dipole's orientation angle, $\theta(t)$, and the

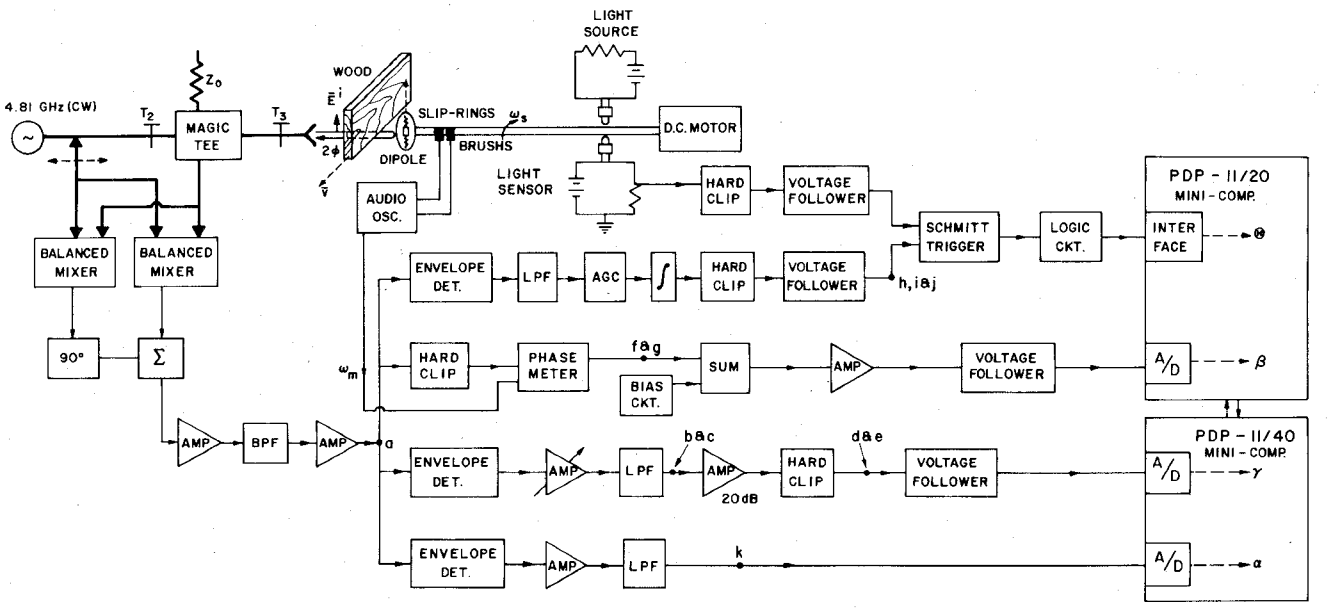

Fig. 3. Entire microwave, analog, and digital system for nondestructive testing of dimension lumber.

anisotropic properties of the wood. The effects of all of these factors are measurable from the information provided in (5).

The combiner output is first amplified (~40 dB) and bandpass filtered to eliminate all components at $2n\omega_s$ ($n=1,2,\cdots$) and $p\omega_m$ ($p=0,2,3,\cdots$). The remaining ($p=1$) component at ω_m is then given by (5), where the filter must have sufficient bandwidth to accommodate all significant frequency components at $\omega_m \pm 2n\omega_s$ (see Appendix). In the present system, we found $n=6$ to be satisfactory so that the bandwidth is 4 kHz for $f_s=150$ Hz. Fig. 4 shows a typical waveform of (5) at point a on Fig. 3, taken in free space with no wood present.

As the dipole spins at ω_s it sweeps out the instantaneous mean-square amplitude $|\boldsymbol{E}\cdot\boldsymbol{u}(t)|^2$ and twice the instantaneous phase, $2\phi(t)$, according to (5). These data are repeated for every 180° of rotation, i.e., at a rate of $2f_s$. Although in principle, the amplitude and phase of the field at the dipole are available at every value of θ, it is generally sufficient to measure only four parameters. These are the values of amplitude along the major and minor axes of the polarization ellipse (denoted as the α and γ branches, respectively, in Fig. 3), the phase along the major axis (the β branch), and the polarization angle (Θ branch). If the field is known to be linearly polarized, the field along the minor axis is zero. Following analog processing, the minicomputer samples the data from each branch and performs the subsequent storage and manipulation.

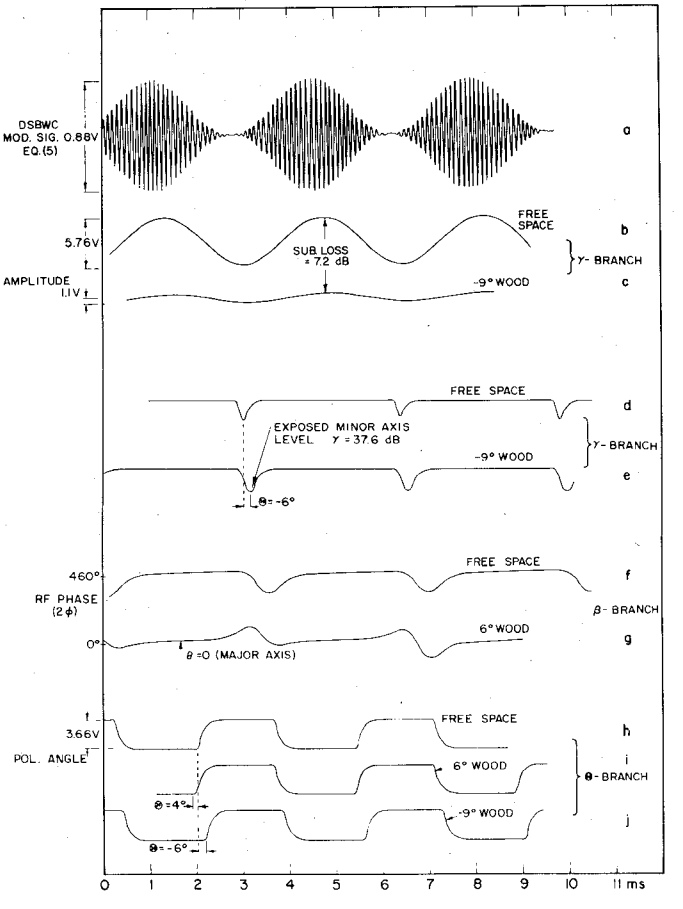

Fig. 4. Typical waveforms measured at the corresponding points a through j in Fig. 3.

α Branch

The peak amplitude of $|\boldsymbol{E}\cdot\boldsymbol{u}(t)|^2=E_{\max}^2$ in (5) occurs when the dipole is aligned along the major axis. It is easily obtained using an ideal envelope detector followed by a low-pass filter designed to eliminate all components of $2\omega_s$ and ω_m. Variations in α correspond to the varying substitution loss. In wood, this loss is primarily a function of moisture content and thickness.

γ Branch

The ratio of the amplitudes at the major and minor axes $\gamma^2=(E_{\max}/E_{\min})^2$, is one of the parameters used to characterize elliptically polarized fields. The amplitude of the major axis is available in the α branch, but determining the

amplitude along the minor axis is considerably more difficult, especially since γ is typically of the order of 15 to 40 dB!

To measure $E^2_{\min}$, the envelope of (5) is again detected using an ideal diode. The low-pass filter eliminates ω_m and all of its higher harmonics, leaving the envelope comprised of $2\omega_s$ and its six harmonics. This envelope is amplified such that $E^2_{\max}$ at b and c in Fig. 3 has the same amplitude as $E^2_{\max}$ at k in the α branch. Two typical waveforms are shown in Fig. 4; b is for no wood present and c is for a $30.5\times19\times4.3$ cm piece of 12-percent moisture content hickory wood with its grain tilted by $-9°$. Comparing the values of $E^2_{\max}$ for b and c, the round-trip substitution loss is 7.2 dB. Normally, however, this loss would be measured in the α branch.

To expose the minimum, the voltage in the γ branch is amplified by another 20 dB and hard clipped, as shown in waveforms d and e. The computer samples this waveform at a 100-kHz rate (every 0.53° for $f_s=150$ Hz), and picks the smallest value of $E^2_{\min}$ out of ten periods; this is repeated ten times, and then averaged and compared with $E^2_{\max}$ from the α branch. γ is then computed after accounting for the 20-dB difference in the two branches.

Obviously, determining γ is very time-consuming; for each value of γ at least 50 revolutions or 0.33 s are needed for $f_s=150$ Hz. Moreover, determining γ becomes more difficult in the presence of noisy $E^2_{\min}$; this becomes a problem when the wood is too lossy, i.e., has high moisture content or is too thick. Mechanical vibrations of the dipole can also contribute significant noise to $E^2_{\min}$.

β Branch

The RF phase, $-2\phi(t)$, is measured at ω_m using an audio phase meter. To stabilize the phase meter input, (5) is hard-clipped to preserve the zero crossings, and compared with the reference modulating voltage from the audio oscillator. The phase meter requires approximately 1.5-ms settling time for $f_m=10$ kHz. Consequently, its output is only accurate during the time when the phase is slowly changing, i.e., in the vicinity of $\theta=0$ or π, corresponding to the phase along the major axis of the polarization ellipse. In the vicinity of the minor axis, the meter loses lock because the phase is changing rapidly and also because the input signal nearly vanishes. Two phase waveforms are shown as f and g in Fig. 4, corresponding to free space and the hickory sample used previously, with the grain tilted $+6°$. The round-trip substitution phase delay of the wood is measured as 460°. The computer is programmed to read and store the β-branch voltage when the dipole is inclined along the major axis, as determined by measuring the axis tilt from vertical, Θ, as discussed below. For wood, the phase is primarily a function of the moisture content and the specific gravity.

Θ Branch

The tilt of the major axis, Θ, is found by measuring the time difference between $E^2_{\max}$ and the reference pulse derived from the light sensor on the motor shaft. The waveform of the amplitude of (5) is detected and then integrated to create a zero crossing at $E_{\max}$. Hard clipping and an automatic gain control amplifier are used to remove the effect of amplitude variations. Resulting waveforms for three cases are compared in Fig. 4, corresponding to free space (h), and the hickory sample of wood with its grain inclined at 6° (i), and at 9° (j) from horizontal. The time displacement of i and j relative to h clearly shows the polarization rotation (Θ) of the transmitted field. Higher moisture content and larger thickness of the wood makes Θ equal to the grain angle.

This waveform and the clipped reference pulses from the light sensor alternatively turn a Schmitt trigger circuit on and off, and the time difference is measured by a logic circuit and stored in the computer.

V. Concluding Remarks

The system is *monostatic* since the backscattered field being measured is received by the same antenna from which it is transmitted. Although the application described here involves transmission through a medium, the system can be used equally well to measure reflected, refracted, or diffracted fields, assuming reciprocity.

It is also possible to measure magnetic fields using spinning loops which are electrically modulated [1]. Furthermore, the system can be readily expanded to accommodate several modulated scatterers (e.g., an array) simultaneously, simply by electrically modulating each scatterer at a different ω_m, i.e., $\omega_{m1}, \omega_{m2}, \cdots$. In this case, each ω_m at the combiner output is selectively filtered and processed in parallel simultaneously. Of course, adjacent ω_m's must be far enough apart so that the bandwidths necessary to accommodate the respective ω_s's do not overlap.

Greater rates of data acquisition are possible by using a higher spinning frequency, ω_s, but this also requires increasing ω_m. In the present system, due to the settling time of the phase meter, a substantial increase in ω_m will permit RF phase measurements over a greater portion of each half of the dipole's rotation. The maximum ω_s is limited by the speed of the computer. For multiple scatterers and hence multiple ω_m's, time-shared data acquisition will be required. Ultimately, dedicated microprocessors are planned for data processing.

Summarizing, the advantages of the system are as follows.

1) Low cost—all microwave components are off-the-shelf items. All signal processing is done at audio frequencies, f_m and f_s.

2) Zero IF permits narrow bandwidths with sensitivities of the order of -120 dBm in a 4-kHz bandwidth for Schottky mixers [1]. The linear dynamic range is of the order of 120 dB.

3) Single-probe antenna is used to measure polarization. Dual receiving antennas and a time-shared receiver are unnecessary, so there is no cross talk and no probe normalization (calibration) is needed. Since the probe is small, probe corrections are minimal or unnecessary. Scattering due to the proximity of the probe ($Z_{11}-Z^0_{11}$) in (A5) is not detected.

4) Probe functions only as a scatterer so no RF circuitry

is needed, e.g., cables, waveguides, mixers, receivers, etc.; these can disturb the field being measured.

5) Coherent detection—phase-lock loops are not needed, and the source frequency, ω, can be swept.

6) Analog amplitude, RF phase, and polarization angle data are available simultaneously and independently in real time. Ultimately, the data rate is limited by the computer.

Some disadvantages and problems to be overcome are as follows.

1) For a high data rate, the scatterer must be spun at a high speed, e.g., 10 to 20 kr/min. Mechanical vibrations then become a problem, particularly when measuring the polarization ratio, $\gamma^2 = (E_{\max}/E_{\min})^2$.

2) γ is the most difficult parameter to measure, and it takes the most computing time because large amounts of data must be averaged to remove slight system instabilities and noise. Fortunately, it turns out that in the present application (testing of wood), γ is much less important than α, β, and Θ.

3) The portion of each half revolution where the dynamic phase can be measured is severely restricted by the settling time of the phase meter. This can be significantly improved by increasing the modulation frequency to 50 or 100 kHz, while still keeping f_s at 150–200 Hz.

Appendix

Backscattering from Modulated Electric Dipoles

The theory and use of modulated scatterers for field measurements has been well documented [1], so we only summarize the salient features for electric dipoles to show the principles as applied to the present system. Magnetic dipoles for measuring $\boldsymbol{H}$ are treated in a similar manner.

Take the transmit–receive and scattering antennas and the intervening medium between them as a two-port network. Then the change in the input (port 1) voltage of the transmit–receive antenna due to the presence of the scattering antenna is

$$V_1 - V_1^0 = \Delta V_1 = \left[\left(Z_{11} - Z_{11}^0 \right) - \frac{Z_{12} Z_{21}}{Z_{22} + Z_L} \right] I_1 \quad \text{(A1)}$$

where Z is the load impedance connected to the scattering antenna terminals (port 2). $Z_{11} = V_{11}/I_1|_{I_2=0}$ is the self-impedance of the transmit–receive antenna and superscript zero implies that the scatterer is removed. Similarly, $Z_{22} = V_{22}/I_2|_{I_1=0}$ is the self-impedance of the scatterer. The mutual impedance is

$$Z_{21} = \frac{-1}{I_1 I_2} \int_{\tau_2} \boldsymbol{E}_1 \cdot \boldsymbol{J}_2 \, d\tau = Z_{12} \quad \text{(A2)}$$

assuming reciprocity. Here, $\boldsymbol{E}_1$ is the field of source 1 when driven by I_1 in the absence of the scatterer and $\boldsymbol{J}_2$ is the current on the scatterer when it is driven with current I_2. Then, if $\boldsymbol{E}_1$ is uniform over the length of the dipole,

$$Z_{21} \cong \frac{-\boldsymbol{E}_1 \cdot \boldsymbol{u} l_e}{I_1} \quad \text{(A3)}$$

where $\boldsymbol{u}$ is the unit vector along the dipole axis (Fig. 1), and the effective length is

$$l_e = \frac{1}{I_2(0)} \int_{l_2} I_2(l) \, dl. \quad \text{(A4)}$$

Thus (A1) reduces to

$$\Delta V_1 = \left(Z_{11} - Z_{11}^0 \right) I_1 - \frac{(\boldsymbol{E}_1 \cdot \boldsymbol{u} l_e)^2}{I_1 (Z_{22} + Z_L)}. \quad \text{(A5)}$$

Important conclusions to be drawn from (A5) are as follows.

a) The quantity $(Z_{11} - Z_{11}^0)$ represents the change in the input impedance of the transmit–receive antenna due to the presence of the scattering antenna. While it varies with position and orientation of the scatterer, it is normally quite small. But more important, it is not electrically modulated at ω_m (although it is modulated at $2\omega_s$). Thus this term is completely eliminated by the narrow-band amplifier which follows the phase-insensitive coherent detector.

b) The second term is modulated both at ω_m (by electronically varying the scatterer's loading impedance Z_L), and at $2\omega_s$ (by varying $\boldsymbol{u}$ through spinning at ω_s, and squaring).

c) The detected voltage is proportional to the phasor $(\boldsymbol{E}_1 \cdot \boldsymbol{u}(t))^2 = |\boldsymbol{E}_1 \cdot \boldsymbol{u}(t)|^2 e^{-j2\phi(t)}$ where $|\boldsymbol{E}_1 \cdot \boldsymbol{u}(t)|$ and $\phi(t)$ are the instantaneous amplitude and phase, respectively, of the component of $\boldsymbol{E}_1$ in the direction of $\boldsymbol{u}(t)$ as the dipole spins at ω_s. Using the phase-insensitive coherent detector shown in Fig. 1, $|\boldsymbol{E}_1 \cdot \boldsymbol{u}(t)|^2$ and $2\phi(t)$ are measured in real time, simultaneously and independently.

d) Taking Z_L as the impedance of a p-i-n diode which is electronically switched between very large and small values at ω_m, the second term in (A5) is modulated double sideband with carrier (DSBWC). The spectrum of the backscattered signal is comprised of the carrier with an evenly distributed cluster of harmonics of $2\omega_s$ due to the first term in (A5), i.e., $\omega \pm 2n\omega_s$. In addition, there are evenly distributed clusters at $\omega \pm (p\omega_m \pm 2n\omega_s)$ due to the second term in (A5), where p and n are integers. Since all but the $\omega_m \pm 2n\omega_s$ components are filtered out after homodyne detection, it is sufficient to consider only this $p = 1$ term. Thus the only relevant component in the DSBWC backscattered voltage appearing at the transmit–receive antenna terminals is the phasor

$$\Delta V = C |\boldsymbol{E}_1 \cdot \boldsymbol{u}(t)|^2 \left[1 + m \cos(\omega_m t) \right] e^{-j2\phi(t)} \quad \text{(A6)}$$

where m is the amplitude-modulation index and C is a constant. Note that this voltage is amplitude modulated at ω_m, and amplitude and phase modulated at ω_s.

References

[1] R. J. King, *Microwave Homodyne Systems*. London, England: Peter Peregrinus Press, 1978

[2] ——, "Apparatus for measuring microwave electromagnetic fields," U S. Patent 4 195 262, Mar 25, 1980.

[3] H. P. Kalmus, "Direction sensitive Doppler device," *Proc. IRE*, vol. 43, pp. 600–700, June 1955.

[4] A. R. Koelle and S. W. Depp, "Doppler radar with cooperative target measures to zero velocity and senses the direction of motion," *Proc. IEEE*, vol. 65, pp. 492–493, Mar. 1977.

[5] A. R. Koelle, S. W. Depp, and R. W. Feyman, "Short range radio telemetry for electronic identification using modulated backscatter," *Proc. IEEE*, vol. 63, pp. 1260–1261, Aug. 1975.
[6] R. J. King, "Error analysis of a phase insensitive coherent (homodyne) detector," submitted to *IEEE Trans. Instrum. Meas.*
[7] ——, "Microwave electromagnetic nondestructive testing of wood," in *Proc. 4th Nondestructive Testing of Wood Sym.* (Vancouver, WA), pp. 121–134.

R. J. King (S'60–M'60–SM'75), photograph and biography not available at the time of publication.

Y. H. Yen, photograph and biography not available at the time of publication.

Short Papers

The Thermal Dielectric Quotient for Characterizing Dielectric Heat Conductors

HAROLD A. WHEELER, FELLOW, IEEE, AND
RICHARD A. LODWIG

Abstract—**If a piece of dielectric is mounted between two conductors, the resulting thermal conductance and electrical capacitance are related by their quotient which is a property of the material, independent of the size and shape. This quotient is expressed in watts per (picofarad × kelvin). It is helpful in the selection of a material for conducting heat while adding least capacitance. For example, a beryllia ceramic block of 1 pF can conduct about 4 W/K. The highest is a diamond of unusual perfection, about 40 W/K. A table and a nomogram give these properties for a variety of materials.**

A dielectric material may also be required to serve as a heat conductor. It may even be added for providing heat conduction at a particular location with the least shunt capacitance. There is proposed a composite rating termed the "thermal dielectric quotient," which has been found helpful in the selection of a material for this purpose.

The thermal dielectric quotient (TDQ$=T$) is defined as the thermal conductance (G) divided by the electrical capacitance (C) in a material filling some space between two conductor faces. The respective field patterns are known to be alike, so this quotient is independent of size and shape. Therefore, it is a property of the material. The TDQ is then equal to the thermal conductivity (K) divided by the electrivity (electrical permittivity). If these are expressed in compatible units (such as the MKS rationalized system) only the essential quantities remain.

$$\mathrm{TDQ}=T\left(\frac{\text{watts}}{\text{picofarads}\times\text{kelvins}}\right)=\frac{G\left(\frac{\text{watts}}{\text{kelvins}}\right)}{C(\text{picofarads})}$$

$$=\frac{K\left(\frac{\text{watts}}{\text{meters}\times\text{kelvins}}\right)}{(8.85\,k)\left(\frac{\text{picofarads}}{\text{meters}}\right)}.$$

TABLE I
THERMAL CONDUCTIVITY CONVERSION FACTORS FOR MKS–KELVIN UNITS FROM OTHER UNITS

Notes:
1 gram-calorie = 4.18 joules
1 BTU = 252 gram-calories = 1055 joules
1 kelvin = 1.8 degrees F

The MKS unit, $\frac{1\ \text{watt}}{\text{meter x kelvin}}$

may alternatively be stated, $\frac{1\ \text{milliwatt}}{\text{mm x kelvin}}$

A.	(CGS)	$1\ \frac{\text{gram-calories}}{\text{seconds x cm x kelvins}}$	$= 418\ \frac{\text{watts}}{\text{meters x kelvins}}$
B.	[6]	$1\ \frac{\text{watts}}{\text{cm x kelvins}}$	$= 100\ \frac{\text{watts}}{\text{meters x kelvins}}$
C.	[8]	$1\ \frac{\text{watts}}{\text{inches x kelvins}}$	$= 39.4\ \frac{\text{watts}}{\text{meters x kelvins}}$
D.	(FPH)	$1\ \frac{\text{BTU}}{\text{hours x feet x degrees F}}$	$= 1.73\ \frac{\text{watts}}{\text{meters x kelvins}}$
E.		$1\ \frac{\text{BTU x inches}}{\text{hours x sq.ft. x degrees F}}$	$= 0.144\ \frac{\text{watts}}{\text{meters x kelvins}}$

The capacitance is expressed in picofarads to give a convenient number; then the electrivity is (8.85 k) pF/m in which k is the material dielectric constant relative to free space. (The kelvin is the most recently adopted term for one degree Kelvin or absolute or Celsius or Centigrade. This unit is strictly not an MKS unit, but is an accepted supplement to that system.)

The simplicity of the units in which the TDQ is expressed is in contrast to the confusion of thermal units in the literature, the only one retained being the temperature difference of the two conductor faces. This simplicity is enabled by assuming faces that are perfect electrical conductors and are perfect thermal conductors. This assumption is valid in some cases, and the TDQ may still be helpful in other cases.

Table I gives, for reference, the factors needed for converting thermal conductivity (K) in various units to the MKS units used herein.

The nomogram in Fig. 1 is chosen for a comparative presentation of the subject properties of typical solid dielectric materials. Each material is represented by a straight line determined by the thermal and electrical properties, which then intersects another scale at the resulting TDQ.

Manuscript received May 11, 1981; revised July 13, 1981. This work was started at Wheeler Laboratories, Inc., Smithtown, NY 11787.

H. A. Wheeler is with Hazeltine Corporation, Greenlawn, NY 11740.
R. A. Lodwig was with Wheeler Laboratories (subsidiary of Hazeltine Corporation), Smithtown, NY. He is now with the Federal Systems Division of International Business Machines, Inc., Gaithersburg, MD 20760.

0018-9480/81/1100-1231$00.75 ©1981 IEEE